SUPPORTING INFORMATION

General Considerations
All reagents were used as purchased from commercial suppliers (Sigma-Aldrich, Strem) without further purification; dried, distilled and deoxygenated solvents were used. Post-synthetic modification (PSM) reactions were performed using standard Schlenk techniques. ^{1}H-NMR, ^{13}C-NMR spectra were taken on Varian XR300 and Bruker 200 spectrometers. Chemical shifts being referred to tetramethylsilane (internal standard).

The solids were characterized by the following techniques:
Elemental analyses were carried out on a Perkin-Elmer CHNS Analyzer 2400 and an Inductively Coupled Plasma Optical Emission Spectroscopy (ICP OES) Perkin Elmer 40 for metal determination.

FTIR spectra were recorded between 4000 and 400 cm^{-1} with a Bruker IFS 66V/S, using the KBr pellets technique (about 1 mg of sample and 300 mg of dry KBr were used in the preparation of pellets).

High resolution **^{13}C MAS or CP/MAS NMR** spectra of powdered samples, were recorded at room temperature under magic angle spinning (MAS) on a Bruker AV-400-WB spectrometer equipped with an FT unit. The ^{13}C cross-polarization (CP-MAS) spectra were acquired by using a contact time of 3.5 ms and recycle of 4 s. All spectra were recorded with a 4 mm ZrO probe and Kel-F plug and at sample spinning rate of 10 kHz.

X-Ray Diffraction (XRD) patterns were performed by a Bruker D8 diffractometer with a Sol-X energy dispersive detector, working at 40 kV and 30 mA and employing CuKα (λ = 1.540 Å) filtered radiation. The diffractograms were registered between 2º and 40º with a step size of 0.02º and exposure time of 0.5 s per step and a 2θ range of 2-40°.

The textural properties were analyzed by N_2 adsorption/desorption experiments performed at -196 ºC using a static volumetric apparatus, Micromeritics ASAP 2010 analyzer. The samples (150–200 mg) were outgassed, previous to the analysis, for 12 h at 80 ºC, or till the outgassing pressure reached 5 mm Hg. For the analysis at low relative pressure range, up to $P/P_0 = 0.05$, successive doses of nitrogen of 4 cm^3 STP/g were added, equilibrating for 1.5 h. Subsequently, the adsorption branch of the isotherm was obtained following a previously fixed 40-points P/P_0 table, and the desorption branch following a previously fixed 20-points P/P_0 table. The specific total surface area was calculated using the Brunauer–Emmett–Teller (BET) method[1], selecting the adsorption data respective to the P/P0 between 0.05 and 0.2 (adjusting the C value from 50 to 150[2]), considering a nitrogen molecule cross-section area value of 0.162 nm^2.[3] The external surface area and micropore volume was obtained by means of the t-plot according to De Boer's method[4]. The total pore volume(Vp) of the solids was estimated from the amount of nitrogen adsorbed at a relative pressure of 0.99, assuming that the densityof the nitrogen condensed in the pores is equal to that of liquid nitrogen at -196 ºC, i.e. 0.81 g/cm^3.[5] The pore size distributions of microporous and mesoporous regions have been performed byusing, respectively, the Horvath–Kawazoe[6] and the Barrett–Joyner–Halenda (BJH) methods[7].

The **thermogravimetric and differential thermal analyses (TGA-DTA)** were performed using Seiko TG/DTA 320U equipment in the temperature range between 25 and 850 ºC in air (100 mL min^{-1} flow) atmosphere and a heating rate of 10 ºC min^{-1}.

X-ray photoelectron spectroscopy (XPS) Photoelectron spectra (XPS) were recorded using an Escalab 200R spectrometer provided with a hemispherical analyzer, operated in a constant pass energy mode and Mg Kα X-ray radiation (h 1253.6 eV) operated at 10 mA and 12 kV.

Synthesis of Zr(BDC–NH$_2$) (UiO-66–NH$_2$)

Synthesis of Zr-based metal-organic framework was performed in a 250 mL round bottom flask using a procedure similar to that previously described[8]. ZrCl$_4$ (0.4 g, 1.7 mmol) in DMF (75 mL) was dispersed by ultrasound at 50-60 ºC, acetic acid (2.85 mL, 850 mmol) was added. A DMF solution (25 mL) of the linker, 2-Aminoterephtalic acid, (0.311 g, 1.7 mmol) was added to the clear solution in an equimolar ratio with regard to ZrCl$_4$; finally, water (0.125 mL, 0.007 mmol) was added to the solution. The tightly capped flask is sonicated at 60 ºC and kept in a bath at 120 ºC under static conditions for 24 h. After 24 h, the solutions were cooled to room temperature and the precipitate was isolated by centrifugation. The solid washed with DMF (10 mL). After standing at room temperature for 2 h, the suspension was centrifuged and the solvent was decanted off. The obtained particles were washed with ethanol several times in the same way as described for washing with DMF. Finally, the solid was dried under reduced pressure (80 ºC, 3 h). This standard washing procedure yielded the materials denoted with "as-synthesized". (Yield: 577 mg). Zr$_6$O$_4$(OH)$_4$(BDC-NH$_2$)$_6$: Calculated: C, 32.87; H, 1.95; N, 4.79. Found: C, 32.09; H, 2.34; N, 4.83%. The materials show particle size of 350-450 nm measured for DLS (Figure S1
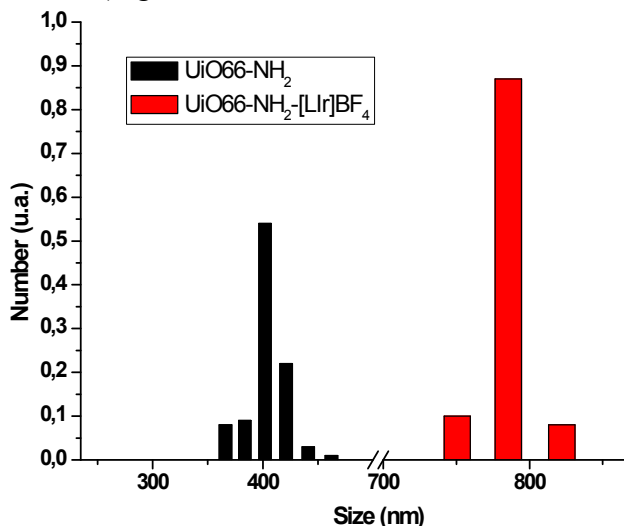

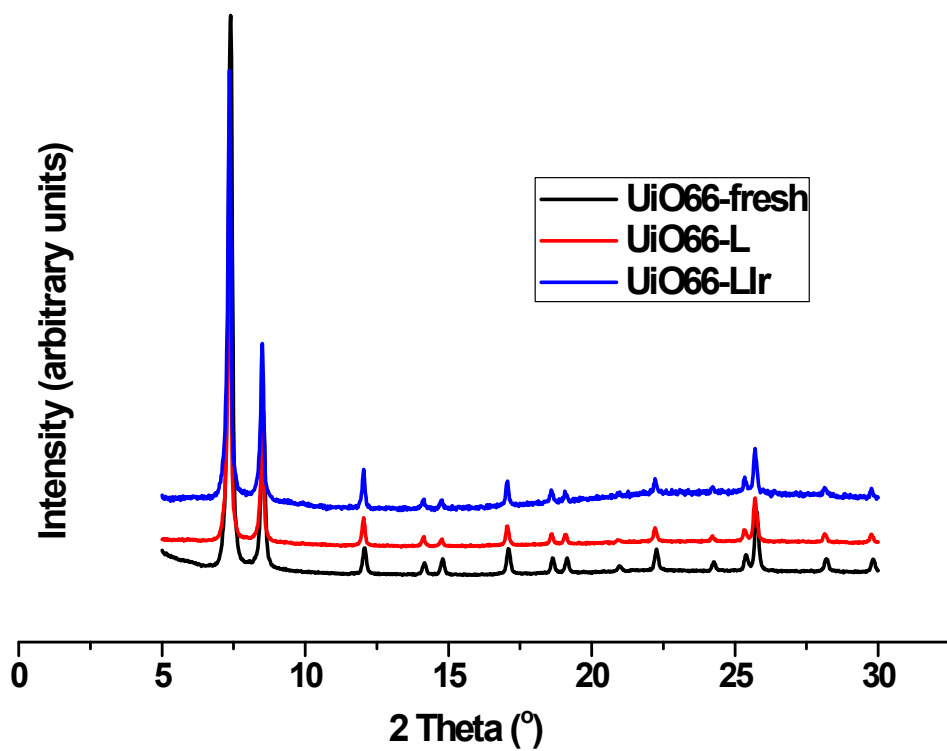Figure S1. DLS measurements of UiO66-NH$_2$ particles.

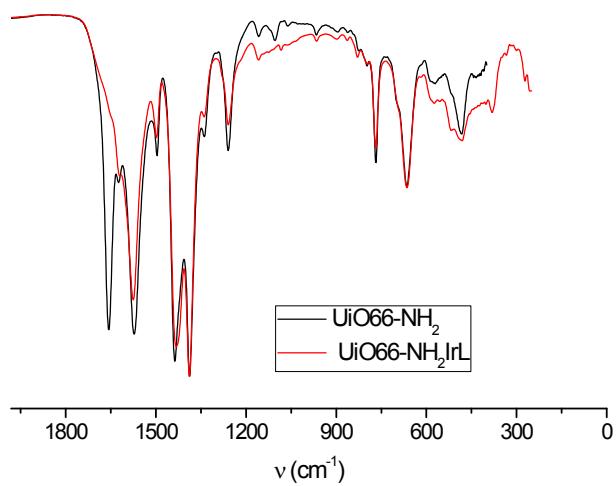Figure S2. PXRD of UiO-66-NH$_2$, UiO-66-NH$_2$-L, UiO-66-NH$_2$-L-Ir.

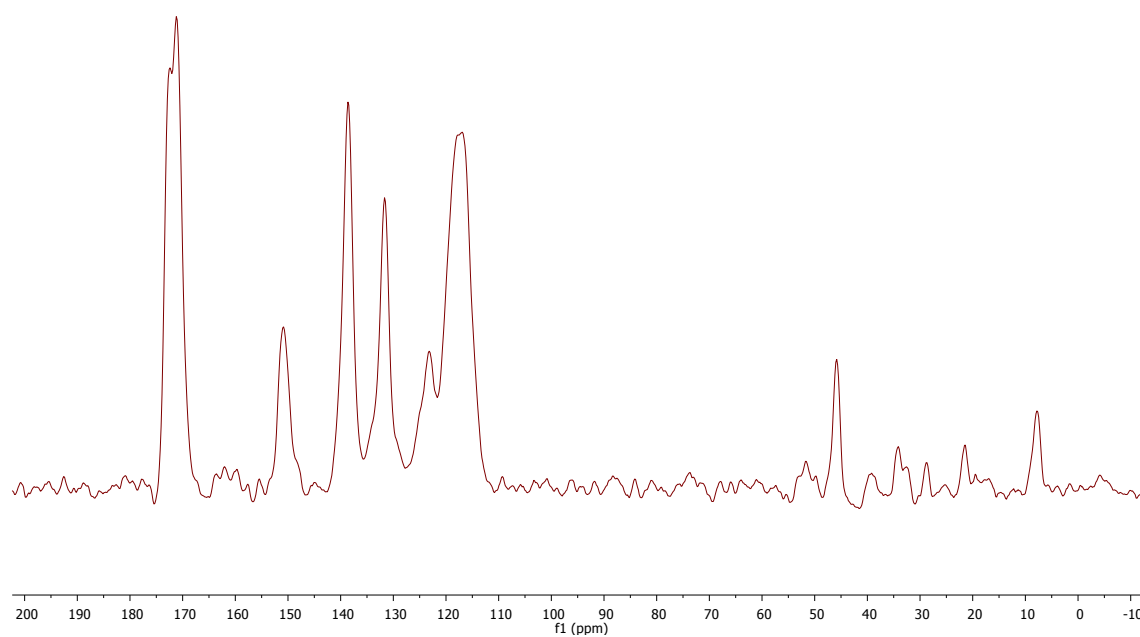Figure S3. FTIR spectra of UiO66-NH$_2$ and the post-synthetic modified UiO66-NH$_2$-L.
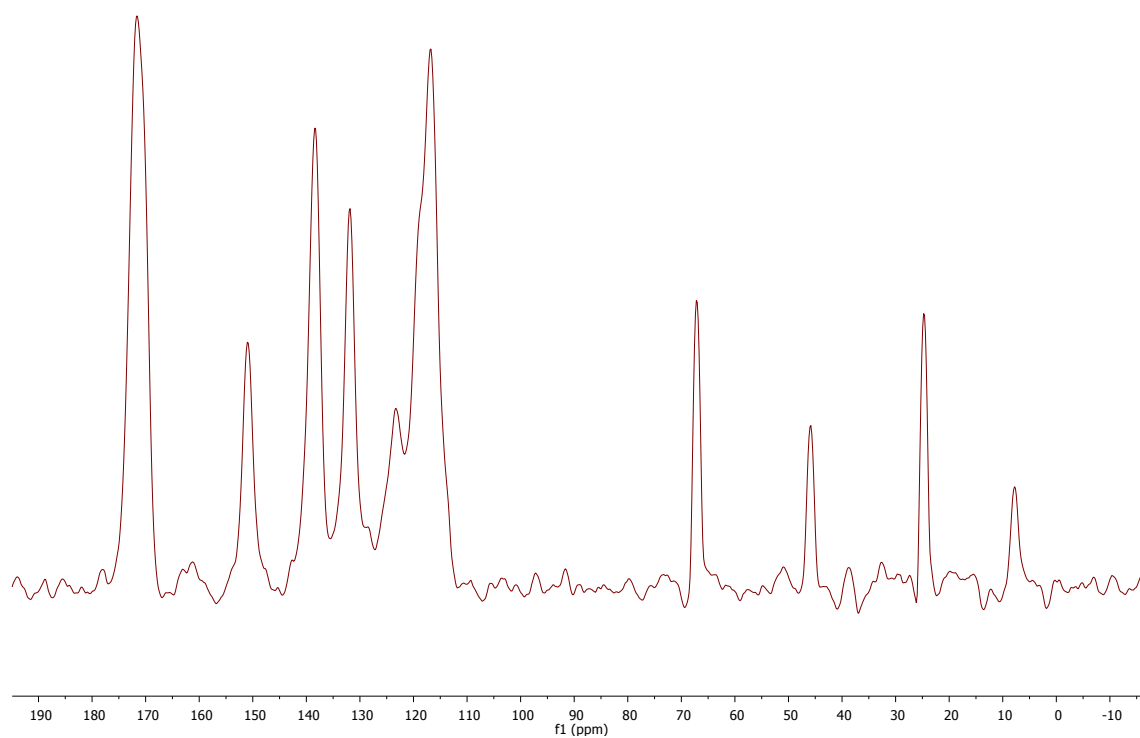
Figure S4- ^{13}C NMR UiO66-NH$_2$-L

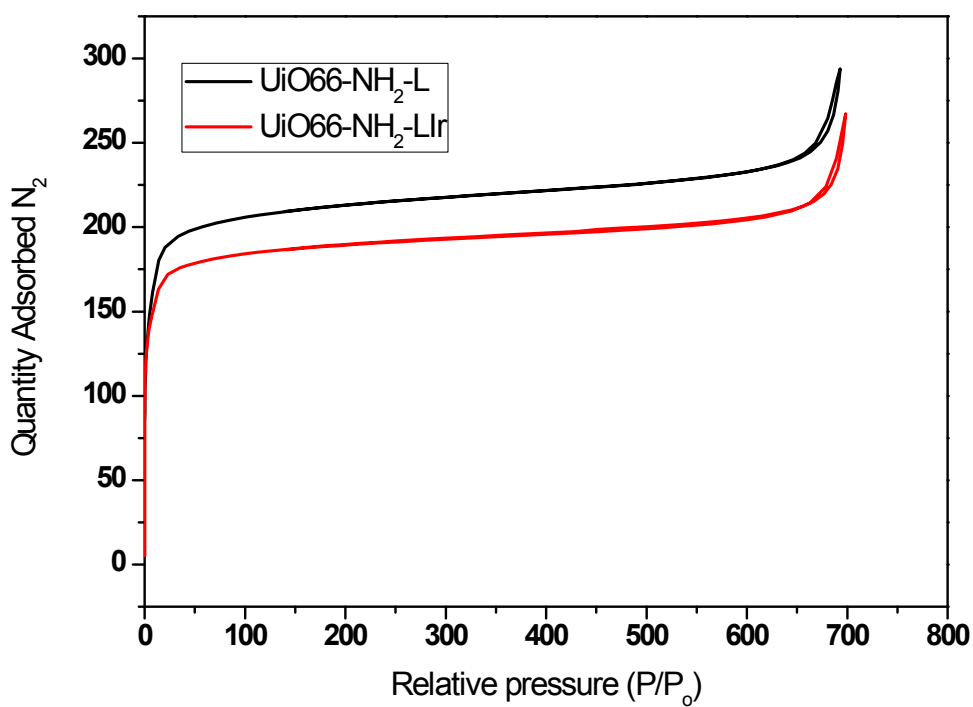Figure S5- ^{13}C NMR UiO66-NH$_2$-LIr

4

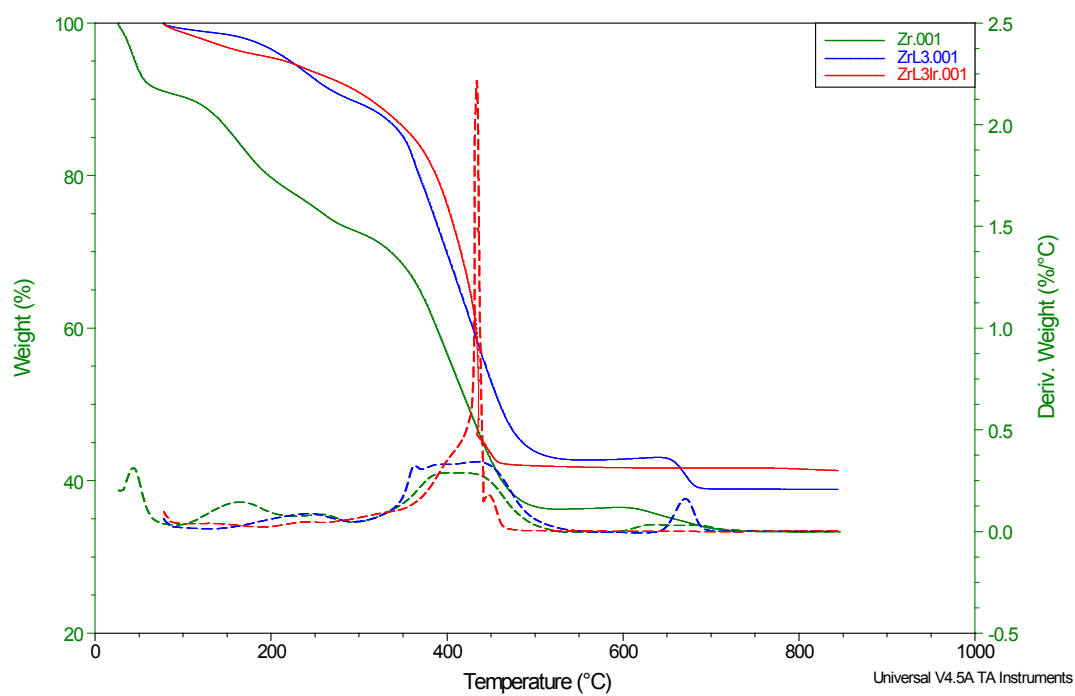Figure S6. The N_2 isotherms (77K) of funcionalized UiO66-NH_2.
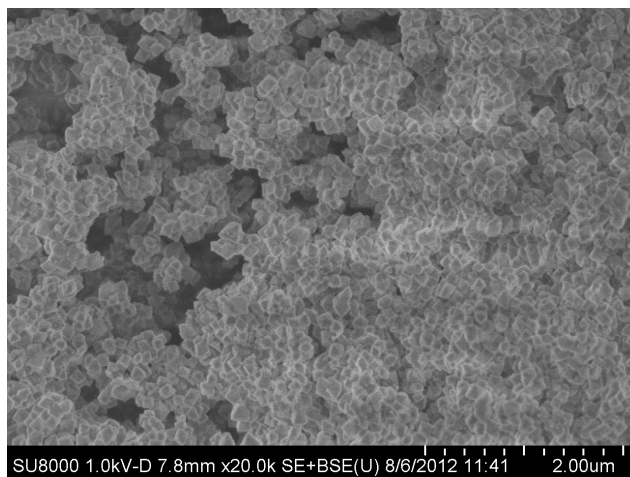

Figure S7. TGA patterns of UiO-66-NH_2, UiO-66-NH_2-L, UiO-66-NH_2-L-Ir.
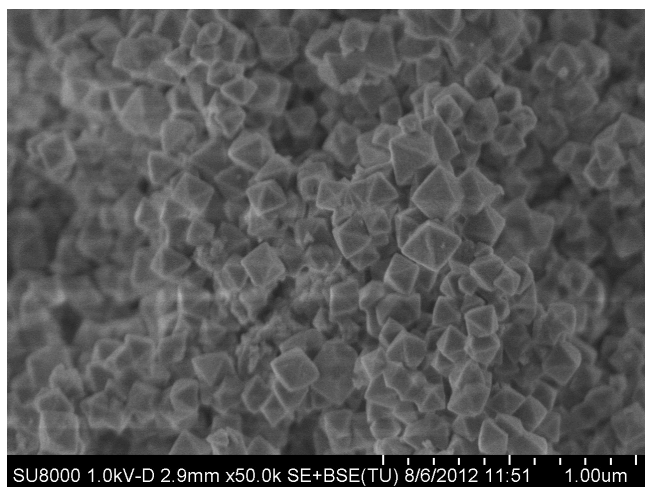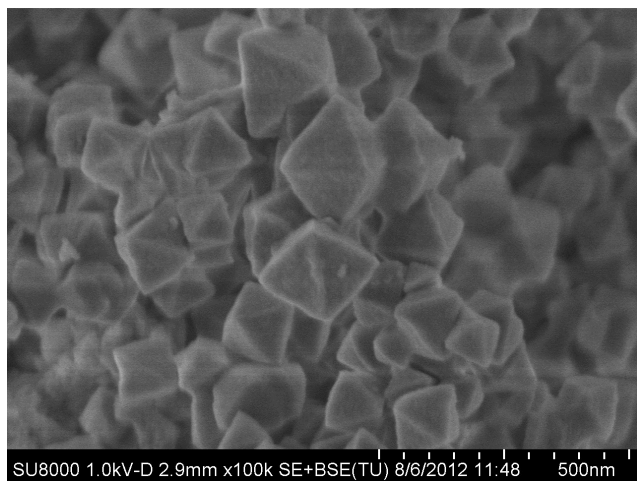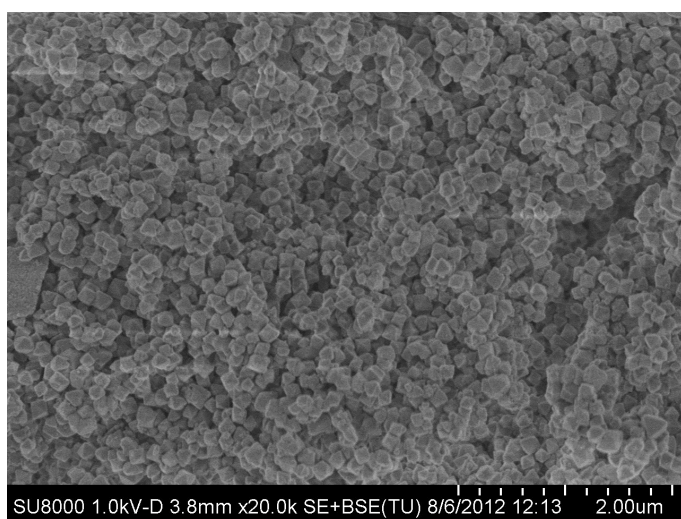
Figure S8.- SEM for UiO66-NH$_2$-L

SU8000 1.0kV-D 2.4mm x100k SE+BSE(TU) 8/6/2012 12:24   500nm

SU8000 1.0kV-D 3.8mm x20.0k SE+BSE(TU) 8/6/2012 12:13   2.00um
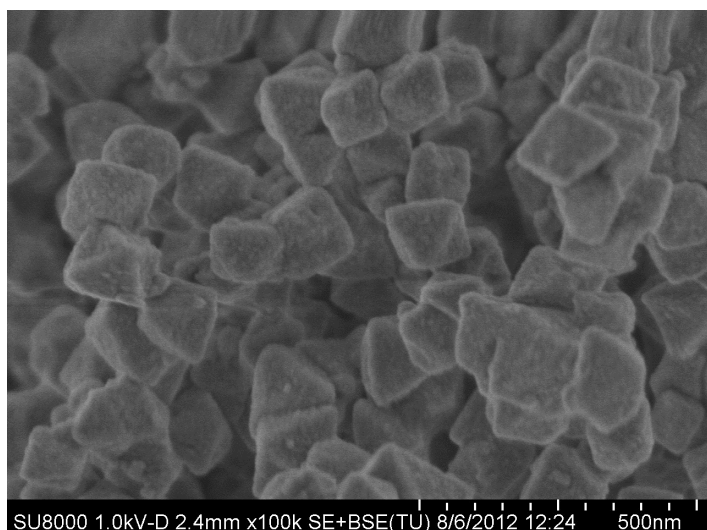
Figure S9.- SEM for UiO66-NH$_2$-[LIr]BF$_4$
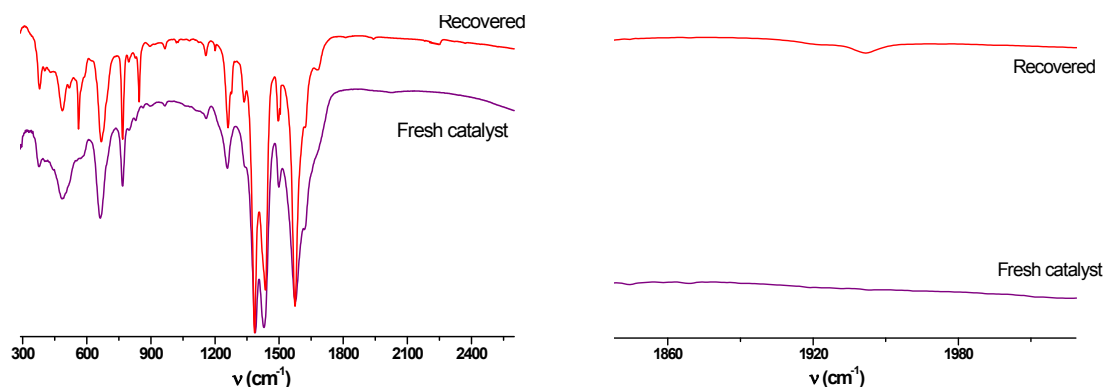
Figure S10. FT-IR of fresh and recovered catalysts after the hydrogenation of aniline.

Morphology

The morphology of the different Ir-Zr-MOF samples was examined by dynamic light scattering (DLS) (Fig. S11), SEM (Fig. S12) and TEM (Fig. S13). SEM images of Zr-[LIr]-MOF fresh obtained reveal particles with diameters between 200 nm and 300 nm; DLS measurements give values of 770 nm (note that DLS measures the hydrodynamic radius including a solvating shell, leading to larger particle sizes than obtained by direct imaging techniques). After reaction SEM images and DLS measurements of the recovered catalyst reveal particles with a similar size to that from fresh one. However, when Zr-[LIr]-MOF reacted with $NaBH_4$ we observe that particle size diminishes (~ 135-150 nm from SEM, 270 nm from DLS). In TEM images, the dark spots could be attributed to the presence of the grafted Iridium sites. Higher resolution images for these large crystallites are difficult to obtain, due to local damage by the electron beam and the fact that the increased thickness of the sample minimizes the contrast between the metal and the support. From TEM images we have measured the Ir particle size and we found (figure S14) that in fresh obtained Zr-[LIr]-MOF catalyst, the size of the iridium particles ranges from 3.5 to 9 nm, whereas after the first run the recovered catalyst shows two patterns for the Ir-particle size: one from 5 to 9 nm and from 19 to 35 nm. Finally for Zr-[LIr]-MOF treated with $NaBH_4$, size ranges mainly between 20-40 nm.
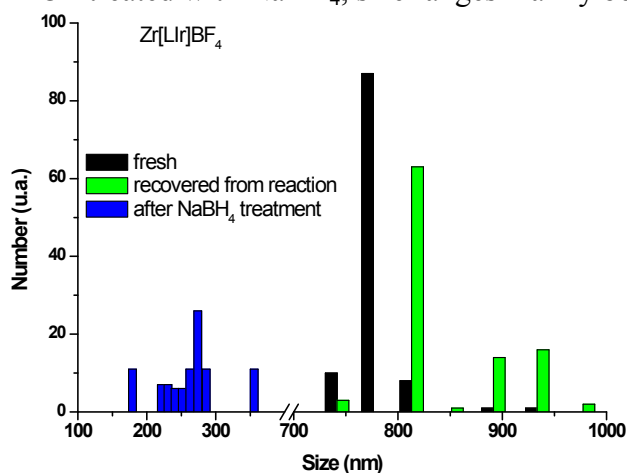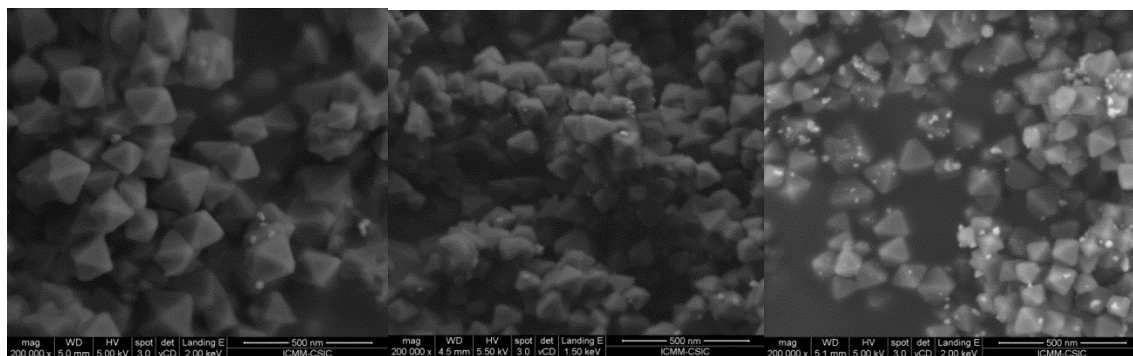

Figure S11. DLS measurements of UiO66-NH$_2$ particles as a function of treatment after synthesis: evolution of the size distribution of the reaction mixture (black: fresh prepared, green: recovered from the aniline hydrogenation, blue: treated with $NaBH_4$).

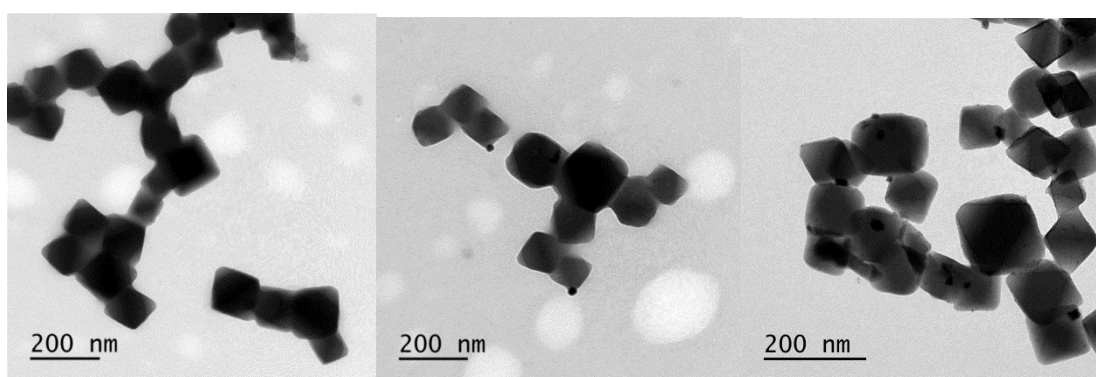a) Fresh   b) recovered after reaction   c) from NaBH$_4$

Figure S12. SEM images for Zr-MOF-Ir samples.

a) Fresh   b) Recovered after reaction   c) 6 bar H$_2$, 120 ºC
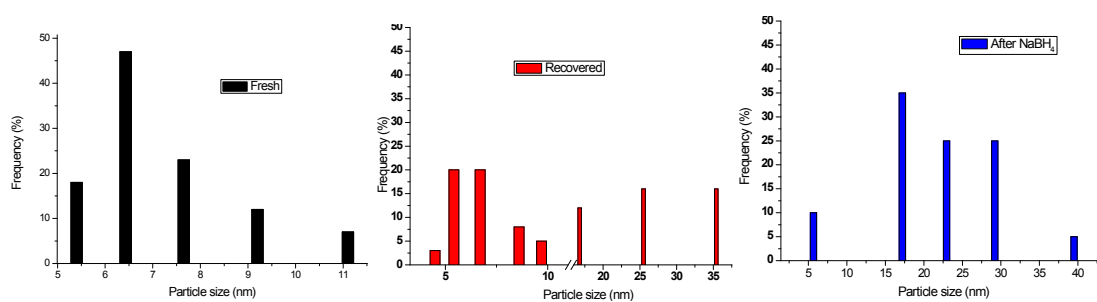
Figure S13. TEM images for Zr-MOF-Ir samples
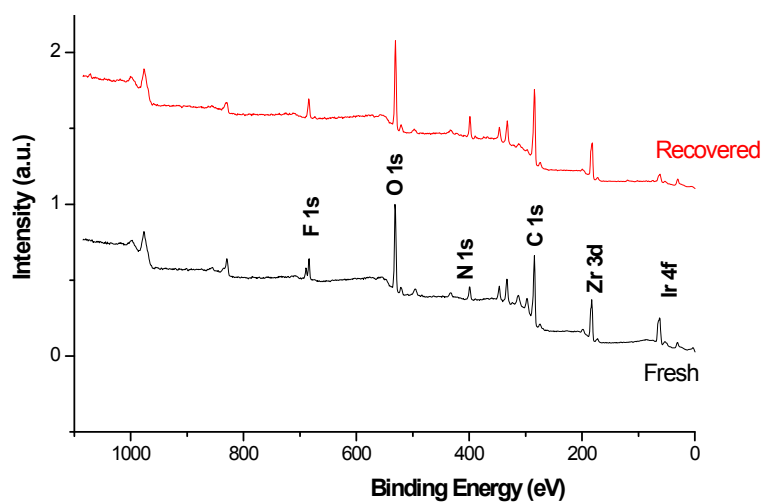

Figure S14. TEM IrNPs size distribution

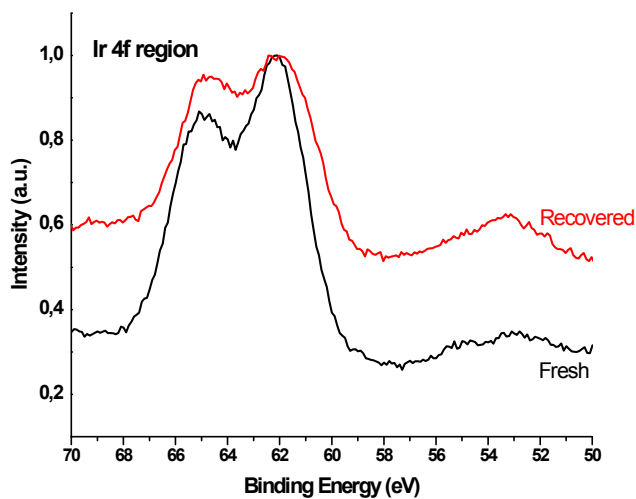Figure S15a. XPS survey scans of a fresh and a used sample after a hydrogenation run.

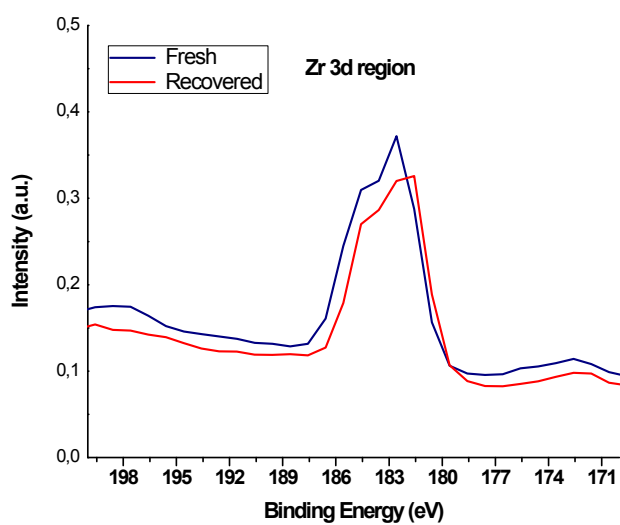Figure S15b. XPS Ir(4f) region for the original catalyst and recovered after reaction.

Figure S15c. XPS Zr(3d) region for the original catalyst and recovered after reaction.
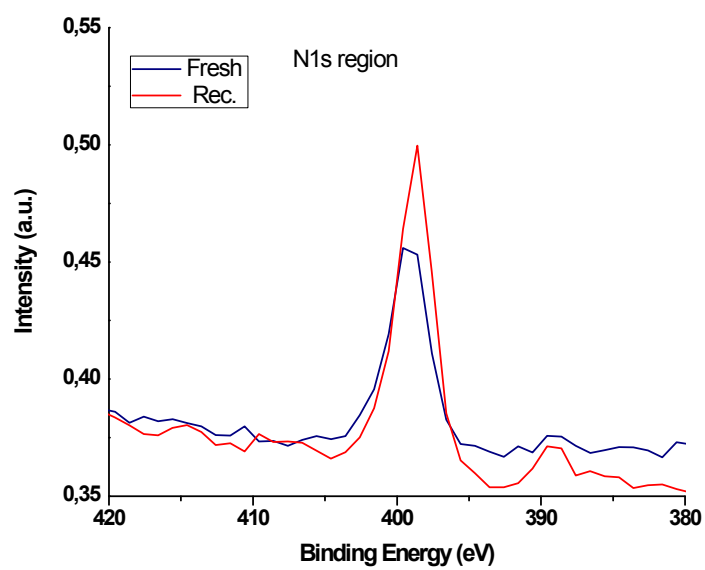
Figure S15d**.** XPS N(1s) region for the original catalyst and recovered after reaction.
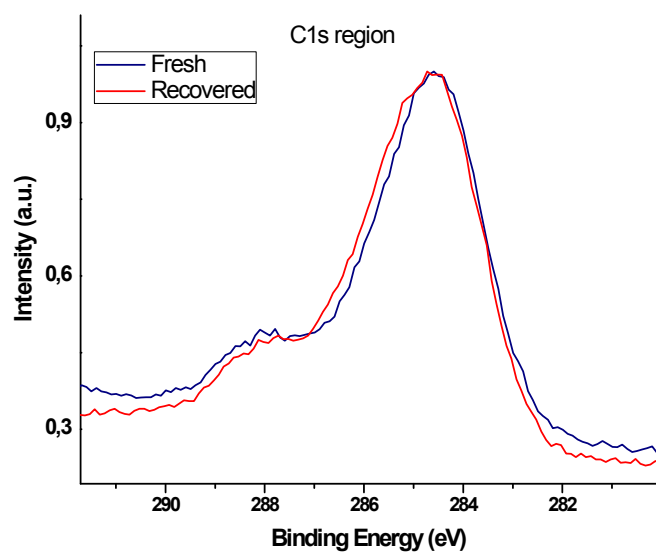

Figure S15e**.** XPS C(1s) region for the original catalyst and recovered after reaction.
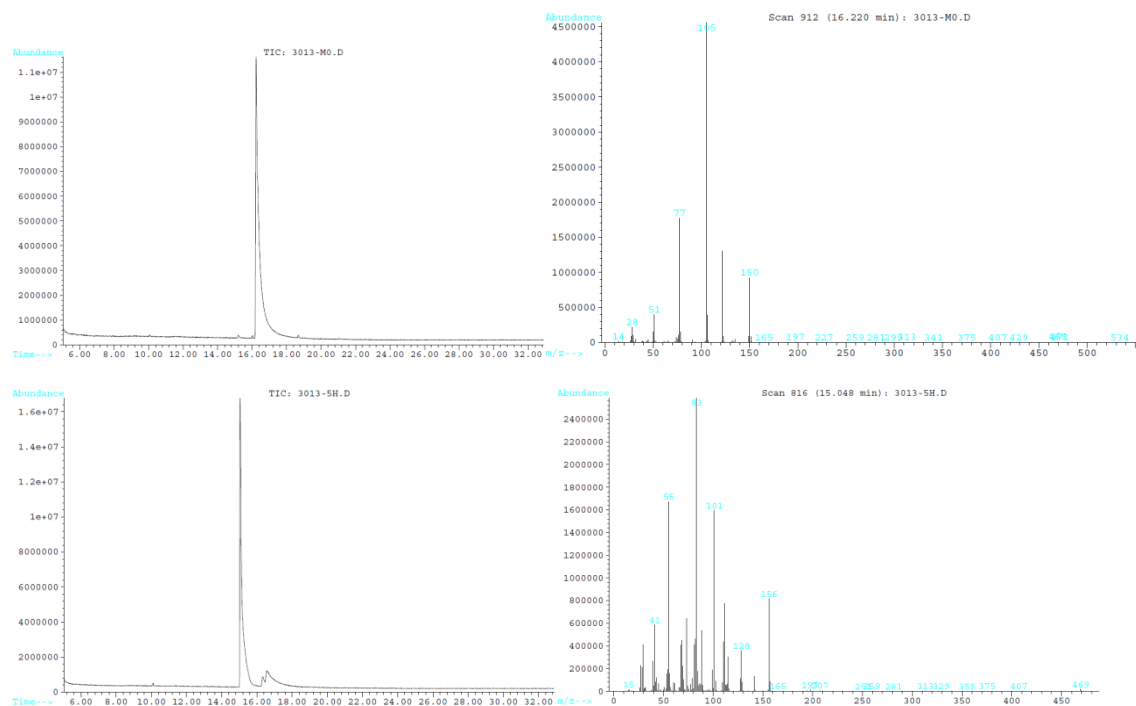
GC-MS traces

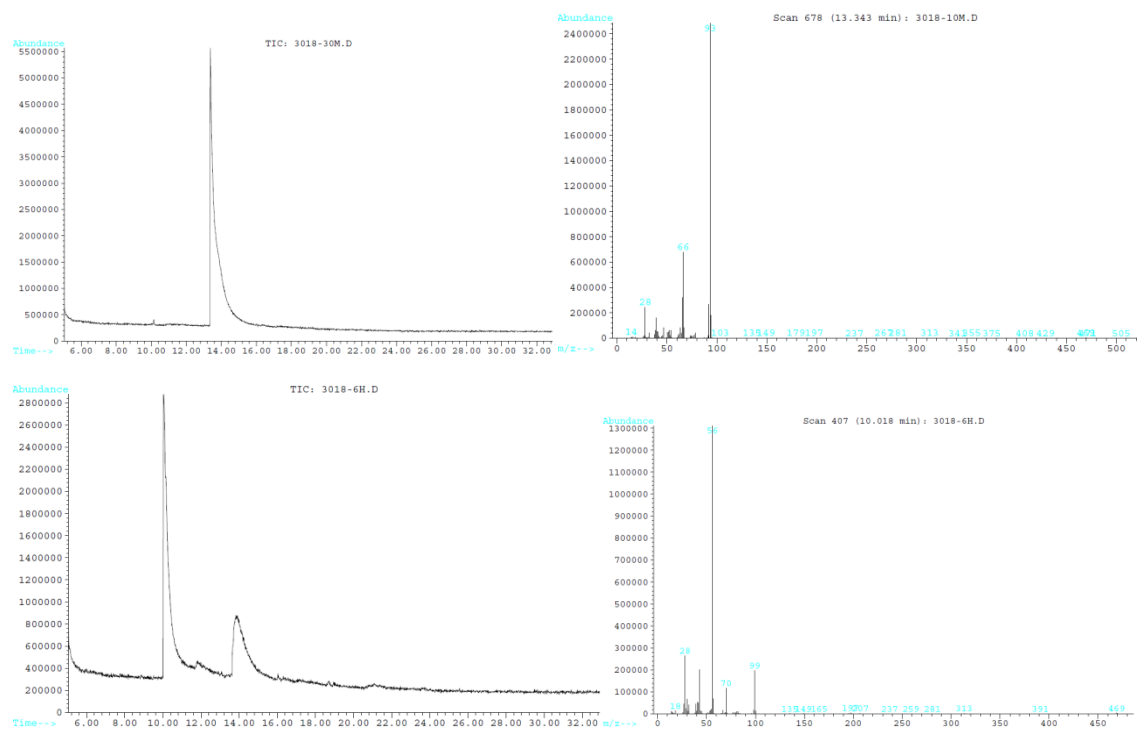Figure S16a. GC-MS analysis for hydrogenation of Ethyl benzoate

Figure S16b. GC-MS analysis for hydrogenation of aniline

[1] S. Brunauer, P.H. Emmett, E. Teller, J. Am. Chem. Soc. 60 (1938) 309–319.

[2] K.S.W. Sing, Colloids Surf. A 187–188 (2001) 3–9.

[3] F. Rouquerol, J. Rouquerol, K.S.W. Sing, Adsorption by powders and porous solids, Principles, Methodology and Applications, Academic Press, London, 1999.

[4] B.C. Lippens, J.H. De Boer, J. Catal. 4 (1965) 319–323.

[5] S.J. Gregg, K.S.W. Sing, Adsorption, Surface Area and Porosity, Academic Press, London, 1982

[6] G. Horvath, K. Kawazoe, J. Chem. Eng. Jpn. 16 (1983) 470–475.

[7] G.P. Barrett, L.G. Joyner, R.H. Halenda, J. Am. Chem. Soc. 73 (1951) 373–380.

[8] A. Schaate, P. Roy, A. Godt, J. Lippke, F. Waltz, M. Wiebcke, P. Behrens Chem Eur J. 17 (2011) 6643-6651